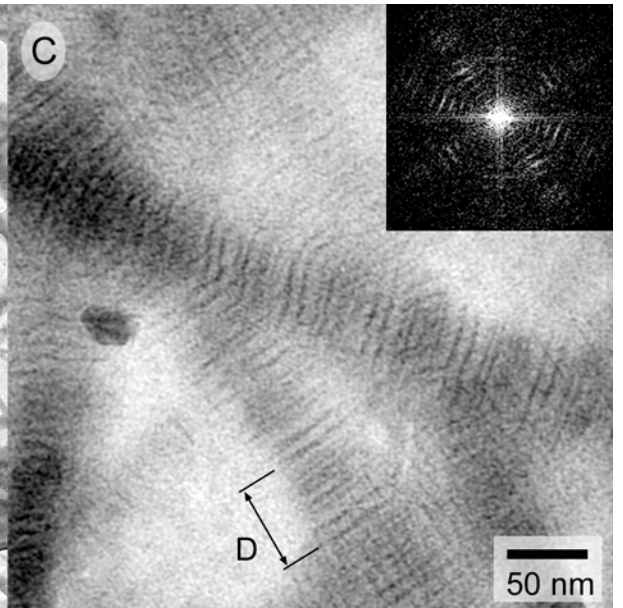
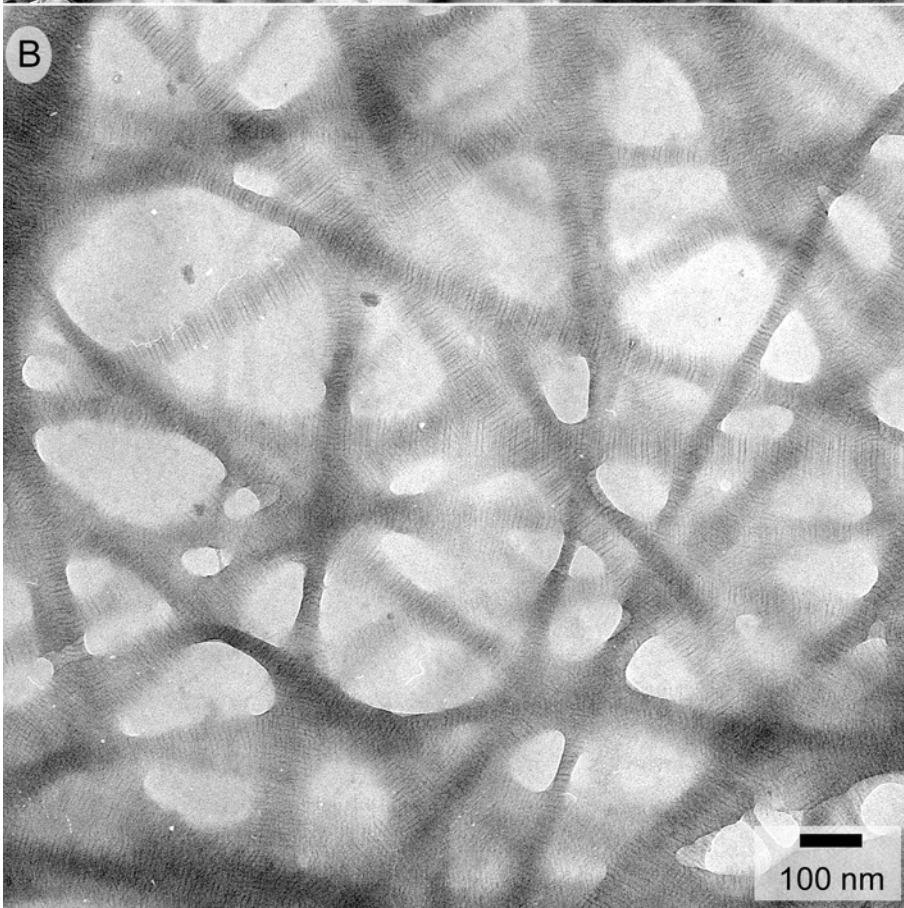
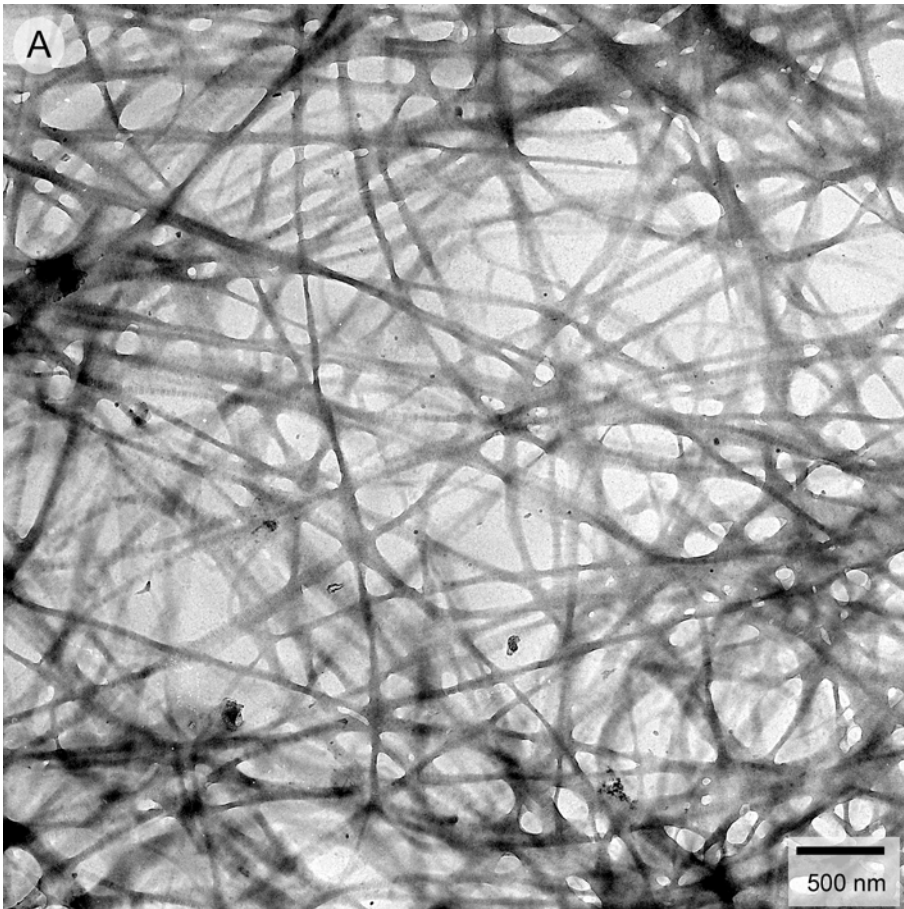
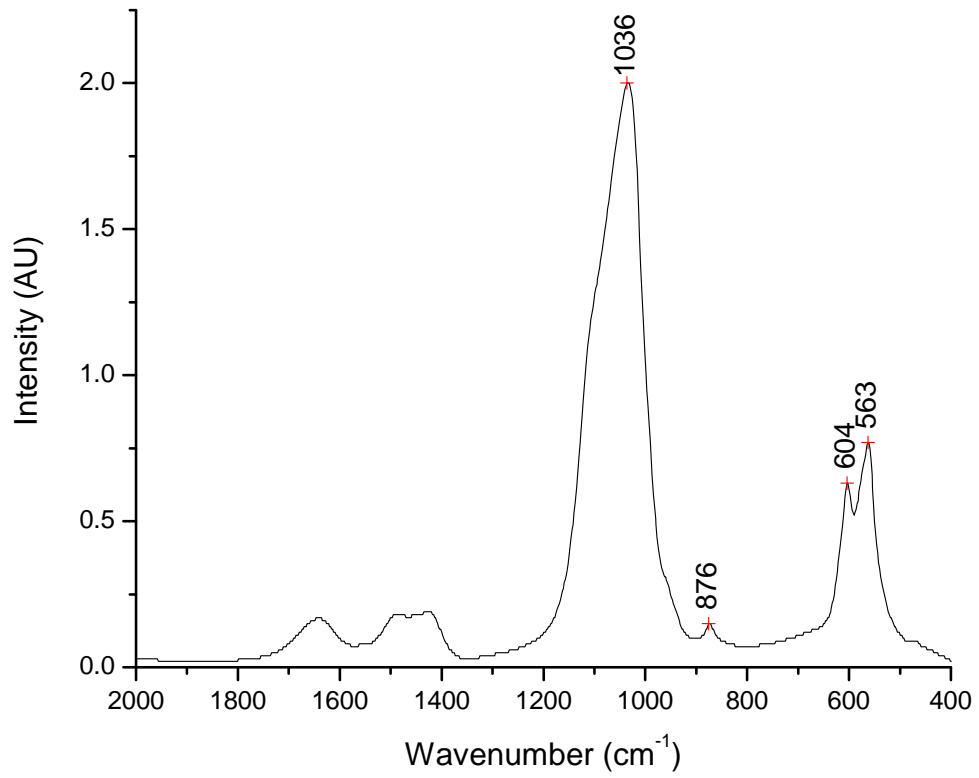


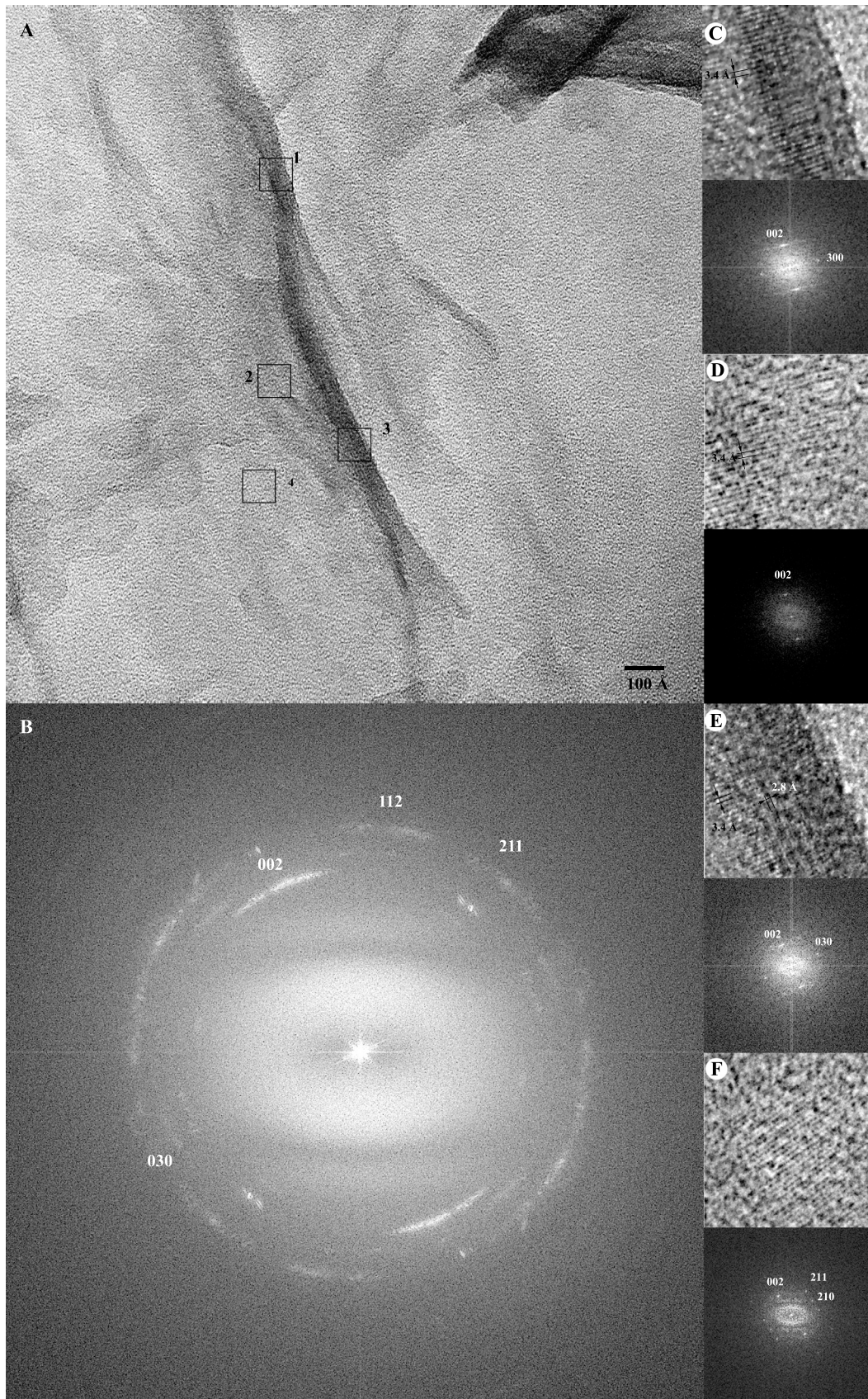
Supplement Figure 1. Purification of DMP1 from MC3T3 cells. A. Western blot of HPLC fractions containing DMP1. B. Determination of protein phosphorylation was conducted using Pro-Q stain (right lane) specifically interacting with phosphorylated amino acids.



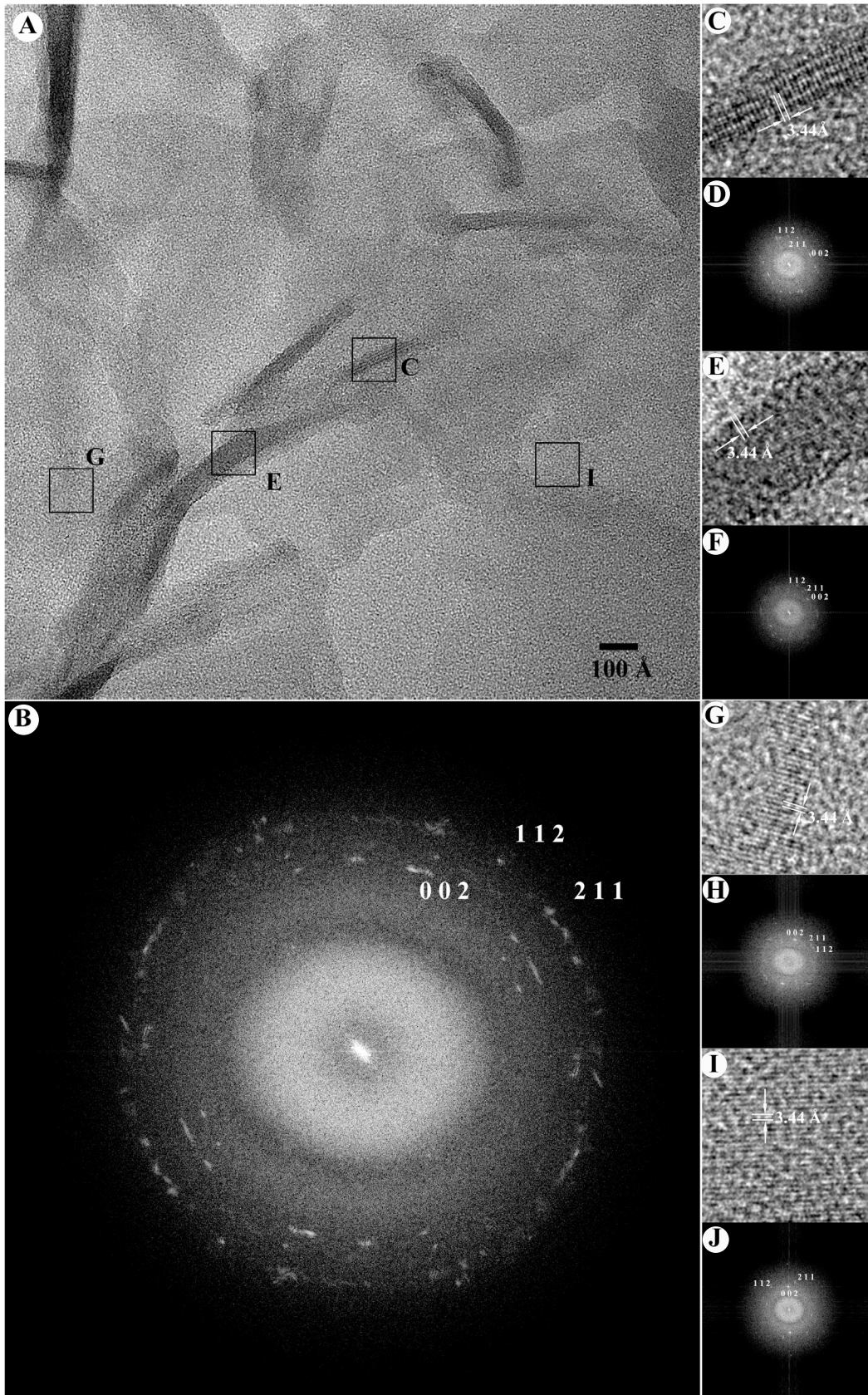
Supplement Figure 2 TEM micrographs of the layers of collagen fibrils positively stained with uranyl acetate at low (A), intermediate (B) and high magnification (C). The fibrils show a banding pattern typical of fibrillar type I collagen in vivo. One D-period of the collagen fibril is highlighted in C. The insert in C represents the power spectrum of the area in the image, showing periodic pattern characteristic of type I fibrillar collagen.



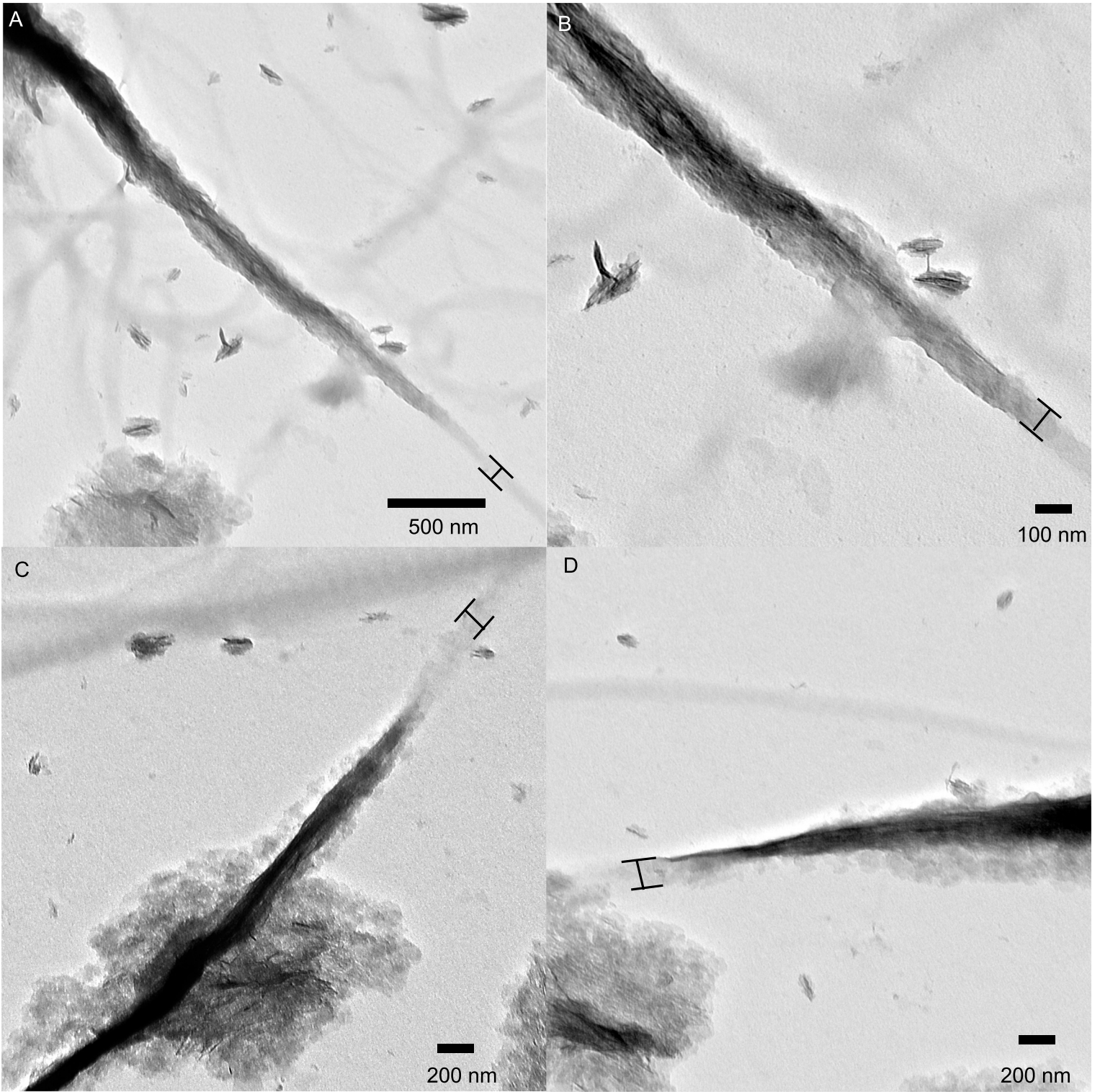
Supplement Figure 3. FTIR spectrum of the control mineral formed without any proteins. Peak at 876 cm⁻¹ corresponds to ν_2 of carbonate, as well as a broad peak in 1500-1400 cm⁻¹ region which corresponds to ν_3 of carbonate. The peak in the 1700-1600 cm⁻¹ region corresponds to water. The split peak with two maxima at 604 and 563 cm⁻¹ is characteristic ν_4 phosphate band of poorly crystalline carbonate apatite, found in bone and dentin. The peak at 1036 cm⁻¹ with the shoulder at 1090 cm⁻¹ is characteristic of ν_4 phosphate vibrations. Overall the spectrum is similar to poorly crystalline carbonate apatite found in mineralized tissues.



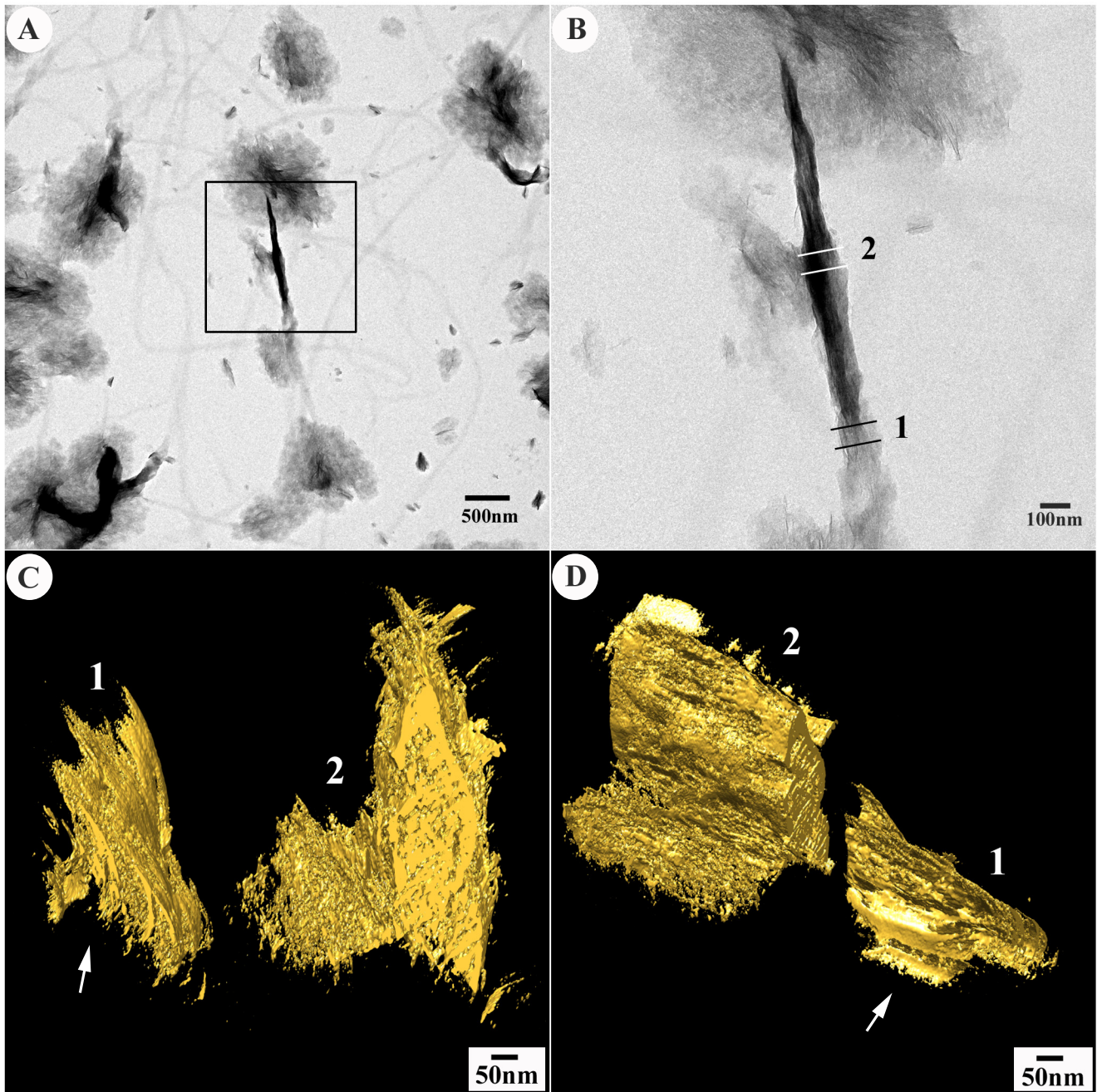
Supplementary Figure 4. HRTEM of the mineral crystals formed in the presence of phosphorylated DMP1. (A) HRTEM micrograph from a mineral aggregate. (B) power spectrum from the area in (A). The numbers correspond to the lattice planes of hydroxyapatite. (C-F) the close up images from squares 1 to 4, respectively and their respective power spectra. The lattice image analysis confirms that the crystals have similar to bone and enamel crystals (Cuisinier, F. J. G. et al. (1992) *J. Cryst. Growth* 116, 314-318.; Cuisinier, F. et al. (1987) *Calcif. Tissue Int.* 40, 332-338)



Supplementary Figure 5. HRTEM of the mineral crystals formed in the presence of phosphorylated DPP. (A) HRTEM micrograph from a mineral aggregate. (B) power spectrum from the area in (A). The numbers correspond to the lattice planes of hydroxyapatite. (C-F) the close up images from squares 1 to 4, respectively and their respective power spectra. The lattice image analysis confirms that the crystals have similar to bone and enamel crystals (Cuisinier, F. J. G. et al. (1992) *J. Cryst. Growth* 116, 314-318.; Cuisinier, F. et al. (1987) *Calcif. Tissue Int.* 40, 332-338)



Supplementary Figure 6. TEM micrographs of collagen fibrils mineralized in the presence of DMP1, in all micrographs the field of view contains both mineralized and nonmineralized portions of collagen fibrils. A and B show the same fibril at low and intermediate magnification. The black lines outline the width of the non-mineralized portions of the fibrils.



Supplement Figure 7. The collagen fibril mineralized in the presence of DMP1, used in the tomographic reconstruction presented in supplementary movie 1. (A) low magnification micrograph of the area, note the mineralized collagen fibril in the box, there are also large mineral aggregates not associated with collagen fibrils. (B) intermediate magnification micrograph of the boxed fibril. C and D Two different projections of tomographically reconstructed sections of the mineralized fibril taken from the areas 1 and 2 in (B). Note that section 1 contains an "imprint" of the collagen fibril (arrows) indicating that the mineral is formed on the surface of the fibril. In section 2 the collagen fibril is partially mineralized. Electron tomography was carried out as described elsewhere (Deshpande, A. S. et al., (2010) *J. Biol. Chem.* 285, 19277-19287; 1. Beniash, E. et al., (2011) *J. Struct. Biol.* 174, 100-106.